J. Am. Soc. Mass Spectrom. (2018) 29:251–259
DOI: 10.1007/s13361-017-1738-4

FOCUS: 32nd ASILOMAR CONFERENCE,
NOVEL INSTRUMENTATION IN MS AND ION MOBILITY: RESEARCH ARTICLE

Quantitative Collision Cross-Sections from FTICR Linewidth Measurements: Improvements in Theory and Experiment

Anupriya, Elaura Gustafson, Daniel N. Mortensen, David V. Dearden

Department of Chemistry and Biochemistry, Brigham Young University, Provo, UT 84602-5700, USA

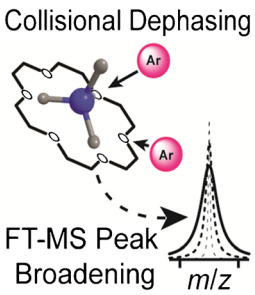

Abstract. Two corrections to the equation used in the cross-sectional areas by Fourier transform ion cyclotron resonance ("CRAFTI") technique are identified. In CRAFTI, ion collision cross-sections are obtained from the pressure-dependent ion linewidths in Fourier transform mass spectra. The effects of these corrections on the accuracy of the cross-sections obtained using the CRAFTI technique are evaluated experimentally using the 20 biogenic amino acids and several crown ether complexes with protonated alkyl monoamines. Good absolute agreement is obtained between the CRAFTI cross-sections and the corresponding cross-sections obtained using both static drift ion mobility spectrometry and computational simulations. These results indicate that the CRAFTI cross-sections obtained using the updated equation presented here are quantitatively descriptive of the size and shape of the gas-phase ions. Cross-sections that differ by less than 3% are measured for the isobaric isomers *n*-butylamine and *tert*-butylamine complexed with the crown ethers. This level of precision is similar to what has been achieved previously using traveling wave ion mobility devices. These results indicate that CRAFTI can be used to probe subtle structural differences between ions with approximately the same precision as that achieved in traveling wave ion mobility devices.

Keywords: Crown ether, Collision cross-section, Fourier transform ion cyclotron resonance

Received: 26 April 2017/Revised: 13 June 2017/Accepted: 14 June 2017/Published Online: 21 July 2017

Introduction

The mobility of ions through inert buffer gases and the corresponding ion collision cross-sections are valuable measures for determining the size and shape of gas-phase ions [1, 2]. The mobility and cross-section of an ion depend on multiple factors, including the shape, mass, and charge state of the ion, the temperature of the buffer gas, and interactions between the ion and the buffer gas [3]. Ions can be separated on the basis of mobility using ion mobility spectrometry (IMS) devices, such as static drift tube [4, 5], traveling-wave [6, 7], field-asymmetric [8, 9], and aspiration [10, 11] type devices. These devices have been used to study a wide range of chemical species, including atomic ions [12, 13], small clusters [13, 14], biopolymers [15–17], and biopolymer complexes [18, 19]. The cross-section of an ion can be obtained directly from the ion drift time in static drift tube devices when all experimental conditions are known or by calibrating the ion drift times in either static drift or traveling wave devices using ions with known collision cross-sections [20–22]. However, in IMS experiments, ions undergo multiple collisions with the buffer gas, and these collisions can induce ion heating and result in conformational changes within the ion [23]. These drawbacks have prompted the development of new methods for determining the collision cross-sections of ions.

Two methods [24, 25] have recently been introduced for determining the cross-sections of ions from the ion linewidths in Fourier transform ion cyclotron resonance (FTICR) mass spectra. These methods are similar, though they differ in data analysis techniques, and have been used to investigate various chemical species, including supramolecular complexes [24, 26], the 20 biogenic amino acids [27], several small peptides [25, 28], and variously charged cytochrome *c* and ubiquitin ions [25, 28]. FTICR linewidth measurement techniques have the advantage that single ion-neutral collisions result in dephasing of the ion packet. Thus, any distortion in ion shape or any ion heating that may occur is not reflected in the resulting collision cross-section value. At high kinetic energies,

Electronic supplementary material The online version of this article (doi:10.1007/s13361-017-1738-4) contains supplementary material, which is available to authorized users.

Correspondence to: David Dearden; *e-mail:* david_dearden@byu.edu

collisions can result in ion dissociation. Ion dissociation changes the cyclotron frequency and removes ions from the coherently orbiting packet necessary for ion detection. Dissociation therefore dampens the time domain signal and broadens the frequency domain linewidth [26]. The relative error in FTICR linewidth measurements also decreases with increasing ion kinetic energy [26]. Therefore, increased analytical performance is generally obtained with increasing ion kinetic energy [26]. Sufficiently massive neutral collision gases should also be used so that single ion-neutral collisions result in complete ion dephasing.

The FTICR linewidth measurement technique used here is known as cross-sectional areas by Fourier transform ion cyclotron resonance mass spectrometry (CRAFTI). Similar trends are generally observed in the ion cross-sections measured using CRAFTI and IMS techniques [24, 27]. However, absolute agreement between these two techniques has thus far been poor [24, 27]. This is partially because in FTICR linewidth measurements, the ions undergo single, relatively high-energy collisions that occur in the hard-sphere collision regime, whereas in IMS, the ions undergo numerous, relatively low-energy collisions that occur in the Langevin collision regime [27]. Because of the low velocity Langevin collisions that occur in IMS, long-range ion-neutral interactions play a significant role in determining the ion collision cross-section, whereas in the high velocity hard-sphere collisions that occur in CRAFTI, long-range ion-neutral interactions play only a small role. Therefore, the cross-sections obtained using CRAFTI should be smaller than the corresponding IMS values. However, we have also recently discovered that two major errors were made while developing the CRAFTI technique. The effects that correcting these errors have on the accuracy of the collision cross-sections obtained using CRAFTI are evaluated using both the 20 biogenic amino acids and several crown ether complexes containing protonated alkyl monoamines. Good absolute agreement is obtained between the cross-sections obtained here using the newly corrected CRAFTI technique and the cross-sections obtained using both static drift IMS and computational simulations. These results suggest that the ion collision cross-sections obtained with the newly corrected CRAFTI technique are quantitatively descriptive of the size and shape of the ions.

Experimental

All experiments were performed using a Bruker model APEX 47e Fourier transform ion cyclotron resonance mass spectrometer with an Infinity trapping cell [29, 30], a micro-electrospray source modified from an Analytica (Branford, MA, USA) design, and a metal capillary drying tube based on the design of Eyler et al. [31]. Data were acquired using a MIDAS Predator data station [32]. Radio frequency (rf) excitation amplitudes were measured using an oscilloscope at the output of the final excitation amplifier. Argon collision gas was introduced into the FTICR cell using a Freiser-type pulsed leak valve [33], and the pressure inside the cell was controlled by varying the duration of the leak valve pressurization event. Absolute pressures in the cell were determined from the Ar^+ linewidths in Ar background gas at each pulsed leak valve pressurization duration, as described in detail elsewhere [34]. Pressure measurements were performed both before and after each CRAFTI measurement, and the average pressures were used in determining the CRAFTI cross-section values.

Procedures for obtaining ion collision cross-sections using the CRAFTI technique are described in detail elsewhere [24]. Briefly, ions are excited with a single-frequency waveform at their resonant frequency in the presence of neutral argon. The full width at half maximum (FWHM) linewidths of the ions in the resulting mass spectra collected at various Ar pressures are obtained from the mass spectra using the Igor Pro software package (ver. 6.37; Wavemetrics, Lake Oswego, OR, USA). Plots of linewidth versus collision gas number density are generally linear, and the slopes obtained from these plots are used to determine the CRAFTI cross-section values.

Molecular mechanics simulations were performed using the Spartan '14 package (Wavefunction, Inc.; Irvine, CA, USA) with the included Merck Molecular Force Field. Conformational searches were conducted for each ion of interest using Spartan's Conformer Distribution module, typically examining 10,000 starting structures or performing an exhaustive search, whichever is smaller. A Boltzmann distribution for the resulting conformers was determined using the relative energies from the minimized force field calculations. The momentum transfer collision cross-section for each of these conformers in helium was determined using the projection approximation and the exact hard sphere scattering methods using the MOBCAL package [35–39]. IMS cross-sections for the crown ether complexes and the amino acids are taken from references [40, 41], respectively. Previously reported CRAFTI cross-sections for the amino acids are taken from reference [27].

Ammonia, *tert*-butylamine, *n*-alkyl monoamines containing between 1 and 9 carbon atoms, 12-crown-4, 15-crown-5, and 18-crown-6 were purchased from Sigma-Aldrich (St. Louis, MO, USA); glacial acetic acid from EMD Millipore (Billerica, MA, USA); HPLC grade methanol from Fisher Scientific (Hampton, NH, USA); HPLC grade water from Avantor (Center Valley, PA, USA); and argon gas (99.995% purity) from Airgas (Radnor, PA, USA). Electrospray solutions were prepared with crown ether and amine concentrations of 100 and 200 μM, respectively, in 49.5/49.5/1 water/methanol/acetic acid.

Theory

The equation used previously to determine CRAFTI collision cross-sections from FWHM linewidths is given in Equation 1:

$$\sigma_{or} = \frac{FWHM}{n_{neutral}} \frac{(m_{ion} + M_{neutral})}{M_{neutral}} \frac{m_{ion}}{q} \frac{d}{\beta V_{pp} t_{exc}} \quad (1)$$

where σ_{or} is the cross-section determined using this original equation, $n_{neutral}$ is the neutral collision gas number density,

m_{ion} and $M_{neutral}$ are the masses of the ion and neutral collision gas, respectively, q is the ion charge, d is the diameter of the FTICR trapping cell, β is the geometry factor for the trapping cell (0.897 for an Infinity cell [30], such as that used here), $V_{p\text{-}p}$ is the peak-to-peak amplitude of the single-frequency rf excitation pulse, and t_{exc} is the duration of the excitation event. Equation 1 was derived in part using the ion-neutral collision rate in a drift ICR device [42] ($\xi_{drift,ICR}$), as described in Equation 2:

$$\xi_{drift,ICR} = \frac{M_{neutral}}{m_{ion} + M_{neutral}} \sigma n_{neutral} v \quad (2)$$

where σ is the ion cross-section and v is the ion velocity. In a drift ICR device, the ion undergoes repeated collisions with the neutral buffer gas (mean free path of perhaps a few cm or less under typical conditions), resulting in a loss of kinetic energy proportional to the reduced mass of the ion-neutral pair. Thus, the ion velocity and ion-neutral collision rate in such a device depends on the reduced mass of the system. However, in CRAFTI experiments, the pressure is typically 4 orders of magnitude lower, such that ions have a mean free path of hundreds of meters. The ions are dephased by single ion-neutral collisions, and the probability of a single ion-neutral collision occurring does not directly depend on mass but rather on the ion velocity, the collision cross-section, and the neutral collision gas number density. Thus, the ion-neutral collision rate in a CRAFTI experiment (ξ_{CRAFTI}) should be written as Equation 3:

$$\xi_{CRAFTI} = \sigma n_{neutral} v \quad (3)$$

Because the reduced mass term is eliminated from the equation describing the collision rate in a CRAFTI experiment, the inverse of this term should also be removed from the CRAFTI equation (Equation 1). This is consistent with the method for obtaining collision cross-sections from FTICR linewidth measurements derived by Xu and co-workers, which also does not depend on the reduced mass of the ion-neutral pair [25, 28].

It was also assumed in deriving Equation 1 that the frequency domain FWHM linewidth is equal to the ion-neutral collision rate, which is essentially the same as the decay constant of the ion transient. This assumption is evaluated here by taking the Fourier transform of synthetic ion transients with different decay constants and comparing those decay constants to the FWHM linewidths in the resulting frequency domain mass spectra. Synthetic ion transients were generated by modeling the decaying ion transients as exponentially damped sine waves, as shown in Equation 4:

$$I_t = I_o e^{-ct} \sin(\omega t) \quad (4)$$

where t is time, I_o and I_t are the ion signal intensities at times 0 and t, respectively, c is the transient decay constant, and ω is the ion cyclotron frequency. The synthetic transients were generated using an ion cyclotron frequency of 198.9 kHz, which is typical for the m/z range we frequently work in and corresponds to m/z 360.4 in a 4.7 T magnetic field. Decay constants of between 25 and 85 Hz were used.

A representative synthetic transient and the frequency domain mass spectrum resulting from the Fourier transformation of this synthetic transient are shown in Figure 1a and b, respectively. The FWHM linewidths obtained from Fourier transformation of the transients are shown in Figure 1c as a function of the decay constants. A linear correlation is observed between the FWHM linewidths and the ion transient decay constants, with a y-intercept of 0 and a slope of 1/π. These results indicate that the collision frequency is not equal to the FWHM linewidth but to the FWHM linewidth multiplied by a factor of π, indicating that an added factor of π should be included in the CRAFTI equation. In sum, the two corrections made here result in the corrected CRAFTI equation:

$$\sigma_{cor} = \frac{FWHM}{n_{neutral}} \frac{m_{ion}}{q} \frac{\pi d}{\beta V_{pp} t_{exc}} \quad (5)$$

where σ_{cor} is the ion collision cross-section calculated using this corrected equation. These corrections make our analysis equivalent to that used by Xu and coworkers [25], except that they extract decay constants by fitting the time domain transient, whereas our approach is to use the frequency domain linewidth.

Results

Corrected Amino Acid Cross-Sections

CRAFTI cross-sections were previously obtained for the 20 biogenic amino acids using Equation 1 and a 1.9 keV laboratory frame kinetic energy. The cross-sections for these amino acids are recalculated here using Equation 5. The argon number densities used to calculate the original CRAFTI cross-sections

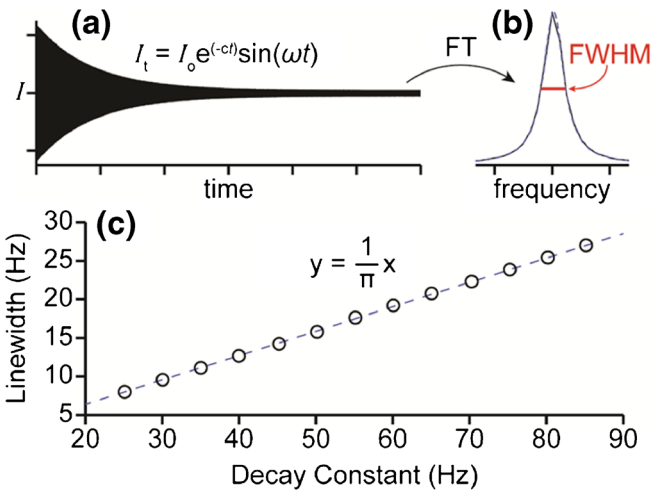

Figure 1. **(a)** A synthetic FTICR ion transient and **(b)** the frequency domain ion peak resulting from Fourier transform of the synthetic transient in **(a)**. The FWHM linewidth is denoted by a red bar. **(c)** Frequency domain FWHM linewidth as a function of the theoretical ion transient decay constant. Dashed lines in **(b)** and **(c)** are Lorentzian and linear fits to the data, respectively

were also measured using FTICR linewidth measurements. Therefore, the values obtained previously for the argon number densities were also corrected on the basis of the errors discussed above. The corrected CRAFTI cross-sections as well as the corresponding IMS cross-sections and cross-sections computed from molecular structures for the amino acids are plotted in Figure 2 and listed in the Supporting Information (Table S-1). Similar cross-sections are obtained using each method and similar trends are observed between all of the different sets of cross-sectional values.

To determine how the corrections made here affect the CRAFTI collision cross-sections and their correlation to IMS cross-sectional values, both the original and newly corrected amino acid CRAFTI cross-sections are plotted as a function of the corresponding IMS cross-sections in Figure 3. The slope obtained between the newly corrected CRAFTI values and the IMS values (1.4) is significantly closer to unity than that obtained between the original CRAFTI values and the IMS values (6.2). The systematic offset of the CRAFTI cross-sections from the IMS values, indicated in Figure 3a as the y-intercept, b, is also ~6 times smaller for the corrected cross-sections (–108) than for the original cross-sections (–596). The CRAFTI cross-sections (which were measured in argon) are also compared with the IMS cross-section values obtained for the amino acids in helium and nitrogen (Figure 3b, green diamonds and grey triangles, respectively). Similar slopes, m, are obtained between the CRAFTI cross-sections and the IMS values measured in helium (1.3), argon (1.4), and nitrogen (1.4). However, a lower systematic offset and a higher R^2 value are obtained with helium (–19 and 0.98, respectively) than with argon (-–108 and 0.93, respectively) or with nitrogen (–125 and 0.89, respectively).

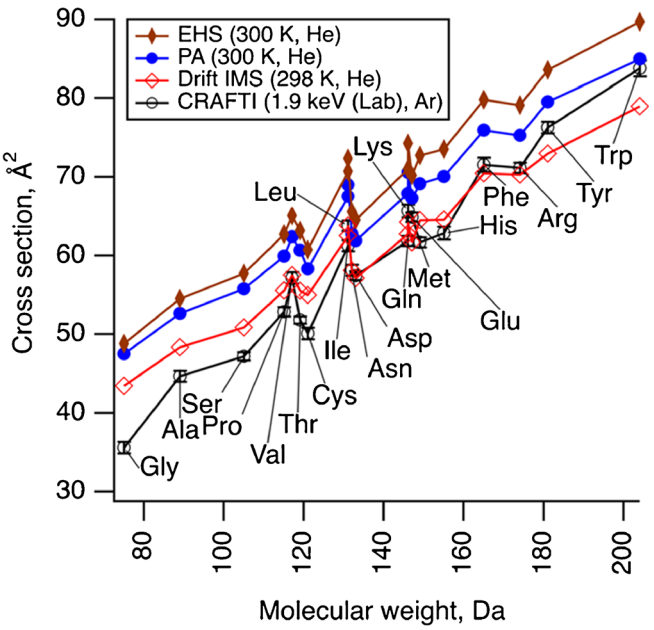

Figure 2. Comparison of cross-sections for the protonated biogenic amino acids determined using computational exact hard sphere scattering (EHS, brown filled diamonds) or projection approximation (PA, blue filled circles) methods [27], drift ion mobility spectrometry (IMS, red open diamonds) [41], and cross-sectional areas by Fourier transform ion cyclotron resonance using Equation 5 (CRAFTI, black open circles). Lines serve only to help in identifying patterns. Note that all values are for cross-sections in He collision gas at thermal energies except those from CRAFTI, which were from 1.9 keV (lab) collisions in Ar

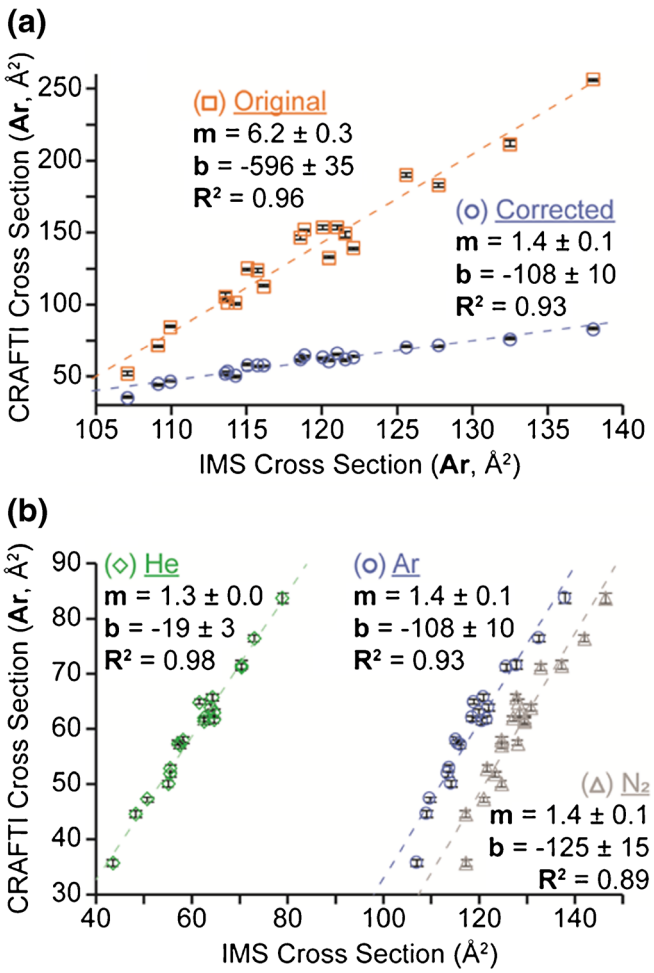

Figure 3. **(a)** CRAFTI collision cross-sections for the 20 biogenic amino acids calculated previously using Equation 1 (orange squares) and the corrected cross-sections for these same amino acids calculated using Equation 5 (blue circles) as a function of the corresponding IMS cross-section values [41]. Data points are mean values of 3 or more measurements, with error bars representing ± one standard deviation. Both the CRAFTI and IMS values in **(a)** were obtained using argon buffer gas. **(b)** Corrected CRAFTI cross-sections for the 20 biogenic amino acids measured in argon as a function of the corresponding IMS cross-sections measured in nitrogen (grey triangles), argon (blue circles), and helium (green squares). Dashed lines are linear fits to the data. Regression statistics are reported in the different panels (m = slope, b = y-intercept, and R^2 = the coefficient of determination)

Cross-Sections of Crown Ether n-Alkyl Monoamine Complexes

To further evaluate the accuracy of the collision cross-sections obtained with the newly corrected CRAFTI Equation (Equation 5), CRAFTI cross-sections were measured for complexes of crown ethers with ammonia and various alkyl monoamines. Crown ether complexes have been extensively studied as model systems for biological host–guest interactions [43–46] and more recently as shift reagents, which complex with peptides and enable the separation of isobaric peptide species using IMS [47]. The crown ethers used here include 12-crown-4, 15-crown-5, and 18-crown-6 (Figure 4a–c, respectively). The amines used include the *n*-alkyl monoamines containing between 1 and 9 carbon atoms and *tert*-butylamine. *Tert*-butylamine was selected because it has the same mass but a different structure and cross-section than *n*-butylamine. Therefore, measuring the CRAFTI cross-sections of the crown ether complexes with these two butylamine isomers will provide a measure of the ability of the CRAFTI technique to distinguish between isomeric structures. The crown ether CRAFTI cross-sections were measured using a constant center-of-mass frame kinetic energy of 130 eV. This energy was selected because it results in good signal intensity for the ions and requires only a short excitation event, which is desirable to minimize the possible influence of collisions during the excitation. Singly-charged 1:1 complexes are observed between the crown ethers and the protonated monoamines. The CRAFTI cross-sections obtained for these different complexes, as well as the corresponding static drift IMS, projection approximation, and exact hard sphere scattering cross-sections, are listed in the Supporting Information (Tables S-2, S-3, and S-4 for the 12-crown-4, 15-crown-5, and 18-crown-6 complexes, respectively).

The CRAFTI cross-sections of the different complexes are shown in Figure 5 as a function of the number of carbon atoms in the amine. For guest ions with the same number of carbon atoms, the cross-sections increase with increasing crown size. Similarly, the cross-sections of the different crown ether complexes increase as the number of methylene groups in the alkyl chain increases. This is consistent with several other studies that show a linear increase in cross-section for homologous compounds as chain length increases [48–51]. For the unbranched amines, the cross-section increases on average by ~6.4, ~6.0, and ~5.2 Å^2 per additional methylene group for the 12-crown-4, 15-crown-5, and 18-crown-6 complexes, respectively, though interestingly on average only about a 2.6 Å^2 difference is observed between the ammonium and methylammonium complexes of each crown ether. Different CRAFTI cross-sections are also obtained for the *n*- and *tert*-butylamine isomer complexes, with the *n*-butyl isomer complexes resulting on average in 3.6 ± 0.3 Å^2 or 2.8 ± 0.2% larger cross-sections than the *tert*-butyl isomer complexes.

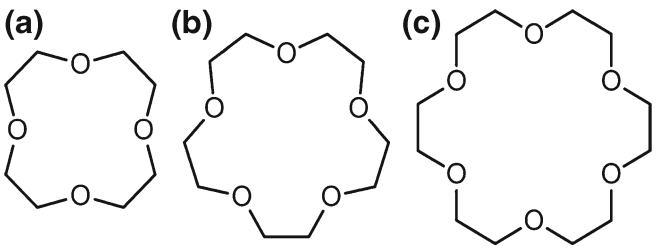

Figure 4. Skeleton formulas of (a) 12-crown-4, (b) 15-crown-5, and (c) 18-crown-6

Discussion

Evaluation of the Corrected CRAFTI Equation

In Figure 3a, the original and corrected CRAFTI cross-sections of the biogenic amino acids are plotted as a function of the corresponding IMS cross-sections. A significant improvement is seen in both the slope and y-intercept obtained between the corrected CRAFTI cross-sections and the IMS values compared with those obtained for the original CRAFTI cross-sections and IMS values. The slope obtained for the corrected amino acid cross-sections (1.4) is substantially closer to unity than that obtained for the original CRAFTI values (6.2). This result suggests that the CRAFTI cross-sections obtained with Equation 5 are significantly more quantitatively descriptive of the three-dimensional shape and size of the ions than the CRAFTI cross-sections obtained previously using Equation 1.

The still significantly large y-intercept obtained for the corrected amino acid cross-sections (–108) likely primarily results from the difference in energy regimes in which collisions occur during CRAFTI and IMS measurements, with the hard-sphere collisions that occur in CRAFTI resulting in smaller cross-sectional values than the Langevin collisions that occur in IMS devices. Support for this idea is obtained by comparing the corrected CRAFTI cross-sections of the biogenic amino acids with the IMS cross-sections of the amino acids measured

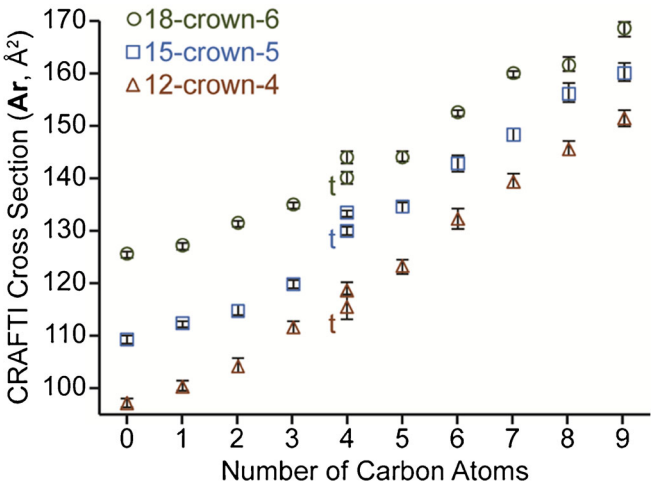

Figure 5. CRAFTI collisional cross-sections of 12-crown-4 (triangles), 15-crown-5 (squares), and 18-crown-6 (circles) complexed with protonated alkyl monoamines as a function of the number of carbon atoms in the amine. All of the alkyl amines are substituted with a single unbranched carbon chain with the exception of *tert*-butylamine, which is denoted by "t"

in nitrogen, argon, and helium (Figure 3b, grey triangles, blue circles, and green diamonds, respectively). The polarizability of helium (1.38 Å^3) [52] is significantly smaller than that of argon (11.07 Å^3) [53, 54] or nitrogen (11.78 Å^3) [53]. Therefore, ion-induced dipole interactions play a significantly smaller role in the collisions that occur with helium than in those that occur with argon or nitrogen. Similar slopes are obtained between the CRAFTI cross-sections and the IMS values measured in helium (1.3), argon (1.4), and nitrogen. However, the systematic offset is nearly 6-fold smaller with helium (–19) than with argon (–108) and nearly 7-fold smaller with helium than with nitrogen (–125). The smaller offset obtained with helium than with argon or nitrogen suggests that long-range ion-induced dipole interactions do not play a significant role in determining CRAFTI collision cross-sections.

Because the van der Waals radius of Ar is about 0.40 Å larger than that of He [55], we would expect to measure larger cross-sections using Ar collision gas than would be observed using He. This is exactly what is seen in IMS experiments at thermal energies. Cross-sections for the protonated amino acids, for example, average about a factor of 2 larger when measured in Ar than when measured in He [41]. Under hard sphere collision conditions, in which ion-induced dipole interactions should not play a large role, we would expect the difference to be smaller. One way to gauge the expected difference is to use the cross-sections computed using the projection approximation, which assume collisions with He, along with the difference in van der Waals radii of He and Ar. If we assume that the rotationally averaged ions are spherical, they will have circular projection approximation cross-sections and we can calculate the radius of the ion+He, r_{He}, from the MOBCAL results ($r_{He} = (\text{cross-section}/\pi)^{1/2}$). We adjust for Ar collision gas by adding the difference Δ in the van der Waals radii of He and Ar to this value, such that the cross-sectional radius in Ar, r_{Ar}, is given by $r_{Ar} = r_{He} + \Delta$, and the cross-section in Ar is just πr_{Ar}^2. For an ion that has a projection approximation cross-section of 100 Å^2 in He, this method yields an estimated cross-section of 114.7 Å^2 in Ar.

Assuming hard sphere collisions, we can get a rough idea of the effect of collision energy on measured cross-sections by examining experimental data for the Ar + Ar$^+$ collision cross-section as a function of energy [56]. At a center-of-mass reference frame collision energy of 5 eV, this cross-section is 94.2 Å^2, but the cross-section falls to 66.5 Å^2 at 119 eV (similar to the energy used for the crown ether experiments) and to only 52 Å^2 at 500 eV (similar to the energies used in the amino acid experiments). Thus, we expect collision energy to play a larger role than the size difference between He and Ar. For the amino acids, the thermal-energy IMS cross-sections in Ar range from about 3 times larger (for Gly) down to about 1.6 times larger (for Trp) than the 1.9 keV (lab frame) cross-sections measured using CRAFTI in Ar (see Supporting Information, Table S-1). The fact that the ratios are smaller for the heavier amino acids likely reflects the decrease in center-of-mass kinetic energies as the amino acid mass increases. Therefore, it is perhaps not surprising that high energy collisions with Ar result in cross-sections that are comparable to or smaller than those computed for thermal collisions with He.

Trends in the Crown Ether Complex Cross-Sections

The cross-sections of the different crown ether complexes increase less per carbon atom as the size of the crown ether increases (Figure 5). Fundamentally, each set of complexes represents a homologous series, with the sets differing only in which "end group" (crown ether) is attached. For homologous sets of compounds, slopes of cross-section versus mass plots have previously been shown to vary based on the identity of the end group [50, 51]. In this case the end groups are quite similar, causing us to wonder why the slopes should vary systematically with crown ether size. This may occur because larger crown ethers have more surface area and are more polarizable than smaller crown ethers and, therefore, have greater dispersion interactions with the alkyl tails of the amines. The more strongly the alkyl tail interacts with the crown ether, the smaller the resulting increase in cross-section with increasing chain length. It is also possible that the larger crowns shield or eclipse the alkyl tails to a greater extent than the smaller crowns.

Interestingly, the difference in cross-section is significantly lower between the ammonium and methylammonium complexes than it is for most of the other complexes that differ in size by a single carbon atom. This is especially true for the 18-crown-6 ammonium and methylammonium complexes, which differ in size by only 1.6 Å^2, whereas for the smaller crowns, the ammonium and methylammonium complexes differ in collision cross-section on average by ~3.2 Å^2.

The small difference in cross-section between the ammonium and methylammonium complexes is likely obtained because the ammonium and methylammonium ions are nested to some extent within the interior of the crown ethers, particularly in the case of 18-crown-6. The longer alkyl chains of the larger alkyl amines protrude more from the crown cavities. This results in the ion cross-sections increasing more rapidly with alkyl chain length for the larger alkyl amines than for the ammonium and methylammonium ions. 18-Crown-6 has a larger interior than the smaller crown ethers and therefore encapsulates the methylammonium ion to a greater extent than occurs for the smaller crown ethers. The 146 pm C–N bond [57] between the amine group and the first methyl group is also slightly shorter than the 153 pm C–C bond [57] that exists between adjacent methyl groups in the alkyl chain. This slightly shorter bond length between the amine and the first methyl group and the encapsulation that occurs for the ammonium and methylammonium ions likely combine to result in the smaller difference in cross-section that is observed between the ammonium and methylammonium complexes than is observed between the other complexes that differ in size by only a single methylene group. Regardless of the correct interpretation, the experimental results are reproducible and demonstrate that small and subtle structural differences between ions can be observed using the CRAFTI technique.

A small difference of 3.6 ± 0.3 Å^2 or 2.8 ± 0.2% (mean ± standard deviation) is also observed between the CRAFTI cross-sections of the *n*- and *tert*-butylamine complexes, with the *n*-butyl complexes being slightly larger. This difference in cross-sections is consistent with the 4.1 ± 1.4 Å^2 and 5.5 ± 2.4 Å^2 differences in cross-section obtained for these complexes using the projection approximation and exact hard sphere scattering computational methods, respectively. Traditional static drift IMS can be used to resolve structures that differ in cross-section by less than 0.1% [58], but traveling wave IMS devices can only resolve structures that differ in cross-section by ~2% or more [7]. These results indicate that CRAFTI may not yet be as precise as static drift measurements, but it can be used to obtain structural information with approximately the same precision as can be achieved using a traveling wave IMS device. It should be noted that in IMS, the ions are separated on the basis of ion mobility, whereas in CRAFTI, isobaric ions of different mobility and cross-section are excited in the same ion packet. It is unclear what result will be obtained from FTICR linewidth measurements when two or more isobaric species are present. Likely it will be an abundance weighted average of the cross-sections of the different isobars, but it is possible that only the cross-section of the largest isobar will be observed.

Accuracy of the Crown Ether CRAFTI Cross-Sections

In order to evaluate how quantitative the CRAFTI cross-sections obtained for the crown ether complexes are, these cross-sections are compared with the cross-sections of these same complexes obtained in nitrogen using static drift IMS [40] (Figure 6a) as well as with those calculated in helium using the projection approximation (Figure 6b) and exact hard sphere scattering (Figure 6c) methods. To the best of our knowledge, IMS cross-sections for these complexes measured in other collision gases have not been reported. Excellent linear agreement (R^2 = 0.98) is observed between the CRAFTI cross-sections and the corresponding IMS values (Figure 6a), with a slope (1.3 ± 0.1) similar to that obtained for the corrected amino acid CRAFTI cross-sections relative to the IMS values (1.4 ± 0.1 and 1.3 ± 0 for argon and helium, respectively). A smaller y-intercept is obtained between the CRAFTI cross-sectional values obtained in Ar and the static drift IMS values obtained in nitrogen for the crown ether complexes (–40, Figure 6a) than for the amino acids (–125, Figure 3b). This may be because of the different collision energies employed in the CRAFTI experiments for the amino acids (constant at 1.9 keV in the laboratory frame, which corresponds to 300–650 eV in the center-of-mass frame, depending on the mass of the amino acid ion) and for the crown ethers (constant at 130 eV in the center-of-mass frame) or it may be because the IMS cross-sections for the amino acids were measured at a lower temperature (300 K) [41] than were the IMS cross-sections for the crown ether complexes (403 K) [40]. The collision cross-sections of ions decrease with increasing temperature [20]. Therefore, the different y-intercepts obtained in Figure 3b (grey triangles) and Figure 6a probably reflect the different energy regimes used in the CRAFTI experiments and/or the different temperatures used in the crown ether and amino acid IMS experiments.

The CRAFTI cross-sections of the crown ether complexes are also assessed by comparing them with the projection approximation (Figure 6b) and exact hard sphere scattering (Figure 6c) cross-sections obtained for these complexes in helium. A linear correlation ($R^2 \geq 0.97$) is observed between the CRAFTI cross-sections and both sets of calculated values. The slopes resulting from both of these linear fits are also near unity (1.2 and 1.1 in Figure 6b and c, respectively), and the y-intercepts resulting from these fits are nearly negligible (–2 and 7, respectively). These results indicate a near 1:1 correlation between the CRAFTI cross-sections and both sets of computationally calculated cross-sections. These results, combined with those in Figure 6a, strongly suggest that the CRAFTI

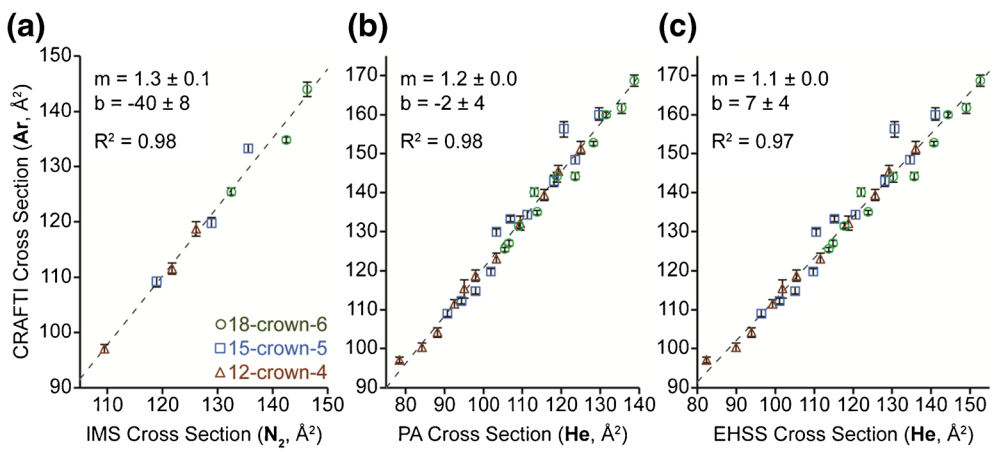

Figure 6. CRAFTI cross-sections for the 12-crown-4 (triangles), 15-crown-5 (squares), and 18-crown-6 (circles) complexes as a function of (a) the corresponding IMS cross-sections measured in nitrogen [40] and the cross-sections calculated using (b) the projection approximation (PA) and (c) the exact hard sphere scattering (EHSS) methods in helium. Dashed lines are linear fits to the data. Regression statistics are reported in the figure (m = slope, b = y-intercept, and R^2 = the coefficient of determination)

cross-sections obtained for these crown ether complexes are quantitatively descriptive of the three-dimensional size and shape of these ions under the collision conditions employed.

Conclusion

Two corrections to the CRAFTI equation are presented here. A strong linear correlation is observed between the CRAFTI cross-sections obtained using this corrected equation and the cross-sections obtained using both static drift IMS and computationally based methods, with slopes near unity. These results strongly suggest that cross-sections obtained using the corrected CRAFTI equation are quantitatively descriptive of the three-dimensional shape and size of the ions. Cross-sections that differ by less than 3% are measured for the *n*- and *tert*-butylamine complexes, demonstrating that CRAFTI can be used to investigate subtle differences in ion structure. This level of precision is similar to that in traveling wave IMS devices, which can resolve structures that differ in collision cross-section by ~2% or more [7], indicating that ion structures can be investigated with approximately the same precision using the CRAFTI technique as is achieved using traveling wave devices. It should be possible to calibrate the CRAFTI-based measurements using ions with known collision cross-sections in order to determine IMS values, such as is commonly done to obtain IMS cross-sections using traveling wave IMS devices. Results from this study also suggest that ion-induced dipole interactions do not play a significant role in determining CRAFTI cross-sections, whereas ion-induced dipole interactions often play a strong role in determining IMS cross-sections, depending on the buffer gas. Therefore, ion structural information may be obtained more readily from CRAFTI cross-sections than from IMS cross-sections for some buffer gases. Further experiments are still required to determine what effects the presence of two or more isobaric species will have on the results obtained from FTICR linewidth measurements.

Associated Content–Supporting Information

Collision cross-sections for the biogenic amino acids measured using the corrected CRAFTI technique presented here and static drift IMS, and collision cross-sections for the 12-crown-4, 15-crown-5, and 18-crown-6 complexes calculated using the projection approximation and the exact hard sphere scattering methods and measured using the corrected CRAFTI technique and static drift IMS.

Acknowledgments

The authors thank Dr. Matthew Asplund for helpful discussions and the National Science Foundation for financial support (CHE-1412289).

References

1. Ferguson, C.N., Gucinski-Ruth, A.C.: Evaluation of ion mobility-mass spectrometry for comparative analysis of monoclonal antibodies. J. Am. Soc. Mass Spectrom. **27**, 822–833 (2016)
2. Lee, H.H., Hong, A., Cho, Y., Kim, S., Kim, W.J., Kim, H.I.: Structural characterization of anticancer drug paclitaxel and its metabolites using ion mobility mass spectrometry and tandem mass spectrometry. J. Am. Soc. Mass Spectrom. **27**, 329–338 (2016)
3. Mason, E.A., McDaniel, E.W.: Transport properties of ions in gases. Wiley, New York (1988)
4. Mcdaniel, E.W., Barnes, W.S., Martin, D.W.: Drift tube mass spectrometer for studies of low-energy ion–molecule reactions. Rev. Sci. Instrum. **33**, 2–6 (1962)
5. Hoaglund, C.S., Valentine, S.J., Sporleder, C.R., Reilly, J.P., Clemmer, D.E.: Three-dimensional ion mobility/TOFMS analysis of electrosprayed biomolecules. Anal. Chem. **70**, 2236–2242 (1998)
6. Giles, K., Williams, J.P., Pringle, S.D., Wildgoose, J.L., Slade, S.E., Thalassinos, K., Bateman, R.H., Bowers, M.T., Scrivens, J.H.: An investigation of the mobility separation of some peptide and protein ions using a new hybrid quadrupole/traveling wave IMS/Oa-ToF instrument. Int. J. Mass Spectrom. **261**, 1–12 (2007)
7. Giles, K., Williams, J.P., Campuzano, I.: Enhancements in Traveling wave ion mobility resolution. Rapid Commun. Mass Spectrom. **25**, 1559–1566 (2011)
8. Purves, R.W., Guevremont, R.: Electrospray ionization high-field asymmetric waveform ion mobility spectrometry-mass spectrometry. Anal. Chem. **71**, 2346–2357 (1999)
9. Shvartsburg, A.A., Li, F.M., Tang, K.Q., Smith, R.D.: High-resolution field asymmetric waveform ion mobility spectrometry using new planar geometry analyzers. Anal. Chem. **78**, 3706–3714 (2006)
10. Räsänen, R., Nousiainen, M., Peräkorpi, K., Sillanpää, M., Polari, L., Anttalainen, O., Utriainen, M.: Determination of gas-phase triacetone triperoxide with aspiration ion mobility spectrometry and gas chromatography-mass spectrometry. Anal. Chim. Acta **623**, 59–65 (2008)
11. Arnanthigo, Y., Anttalainen, O., Safaei, Z., Sillanpää, M.: Sniff-testing for indoor air contaminants from new buildings environment detecting by aspiration-type ion mobility spectrometry. Int. J. Ion Mobil. Spectrom. **19**, 15–30 (2016)
12. Cohen, M.J., Karasek, F.W.: Plasma chromatography – a new dimension for gas chromatography and mass spectrometry. J. Chromatogr. Sci. **8**, 330–337 (1970)
13. Bowers, M.T., Kemper, P.R., Vonhelden, G., Vankoppen, P.A.M.: Gas-phase ion chromatography – transition-metal state selection and carbon cluster formation. Science **260**, 1446–1451 (1993)
14. Jarrold, M.F.: Drift-tube studies of atomic clusters. J. Phys. Chem. **99**, 11–21 (1995)
15. Shelimov, K.B., Clemmer, D.E., Hudgins, R.R., Jarrold, M.F.: Protein structure in vacuo: gas-phase conformations of BPTI and cytochrome *c*. J. Am. Chem. Soc. **119**, 2240–2248 (1997)
16. Thalassinos, K., Slade, S.E., Jennings, K.R., Scrivens, J.H., Giles, K., Wildgoose, J., Hoyes, J., Bateman, R.H., Bowers, M.T.: Ion mobility mass spectrometry of proteins in a modified commercial mass spectrometer. Int. J. Mass Spectrom. **236**, 55–63 (2004)
17. Shi, L., Holliday, A.E., Glover, M.S., Ewing, M.A., Russell, D.H., Clemmer, D.E.: Ion mobility-mass spectrometry reveals the energetics of intermediates that guide polyproline folding. J. Am. Soc. Mass Spectrom. **27**, 22–30 (2016)
18. Ruotolo, B.T., Giles, K., Campuzano, I., Sandercock, A.M., Bateman, R.H., Robinson, C.V.: Evidence for macromolecular protein rings in the absence of bulk water. Science **310**, 1658–1661 (2005)
19. Uetrecht, C., Versluis, C., Watts, N.R., Wingfield, P.T., Steven, A.C., Heck, A.J.R.: Stability and shape of hepatitis B virus capsids in vacuo. Angew. Chem. Int. Ed. **47**, 6247–6251 (2008)
20. Wyttenbach, T., von Helden, G., Batka Jr., J.J., Carlat, D., Bowers, M.T.: Effect of the long-range potential on ion mobility measurements. J. Am. Soc. Mass Spectrom. **8**, 275–282 (1997)
21. Ruotolo, B.T., Benesch, J.L.P., Sandercock, A.M., Hyung, S., Robinson, C.V.: Ion mobility-mass spectrometry analysis of large protein complexes. Nat. Protoc. **3**, 1139–1152 (2008)

22. Bohrer, B.C., Merenbloom, S.I., Koeniger, S.L., Hilderbrand, A.E., Clemmer, D.E.: Biomolecule analysis by ion mobility spectrometry. Ann. Rev. Anal. Chem. **1**, 293–327 (2008)
23. Merenbloom, S.I., Flick, T.G., Williams, E.R.: How hot are your ions in TWAVE ion mobility spectrometry? J. Am. Soc. Mass Spectrom. **23**, 553–562 (2012)
24. Yang, F., Voelkel, J.E., Dearden, D.V.: Collision cross-sectional areas from analysis of Fourier transform ion cyclotron resonance line width: a new method for characterizing molecular structure. Anal. Chem. **84**, 4851–4857 (2012)
25. Mao, L., Chen, Y., Xin, Y., Chen, Y., Zheng, L., Kaiser, N.K., Marshall, A.G., Xu, W.: Collision cross-section measurements for biomolecules within a high-resolution Fourier transform ion cyclotron resonance cell. Anal. Chem. **87**, 4072–4075 (2015)
26. Yang, F., Jones, C.A., Dearden, D.V.: Effects of kinetic energy and collision gas on measurement of cross-sections by Fourier transform ion cyclotron resonance mass spectrometry. Int. J. Mass Spectrom. **378**, 143–150 (2015)
27. Anupriya, Jones, C.A., Dearden, D.V.: Collision cross-sections for 20 protonated amino acids: Fourier transform ion cyclotron resonance and ion mobility results. J. Am. Soc. Mass Spectrom. **27**, 1366–1375 (2016)
28. Jiang, T., Chen, Y., Mao, L., Marshall, A.G., Xu, W.: Extracting biomolecule collision cross-sections from the high-resolution FT-ICR mass spectral linewidths. Phys. Chem. Chem. Phys. **18**, 713–717 (2016)
29. Caravatti, P., Allemann, M.: The 'Infinity Cell': a new trapped-ion cell with radiofrequency covered trapping electrodes for Fourier transform ion cyclotron resonance mass spectrometry. Org. Mass Spectrom. **26**, 514–518 (1991)
30. Sievers, H., Grutzmacher, H., Caravatti, P.: The geometrical factor of infinitely long cylindrical ICR cells for collision energy-resolved mass spectrometry: appearance energies of EI(2)(+) (E = P, as, Sb, and Bi) from collision-induced dissociation of EI(3)(+center dot) and [EI(2)center dot ligand](+) complexes. Int. J. Mass Spectrom. Ion Process. **157**, 233–247 (1996)
31. Wigger, M., Nawrocki, J.P., Watson, C.H., Eyler, J.R., Benner, S.A.: Assessing enzyme substrate specificity using combinatorial libraries and electrospray ionization Fourier transform ion cyclotron resonance mass spectrometry. Rapid Commun. Mass Spectrom. **11**, 1749–1752 (1997)
32. Blakney, G.T., Hendrickson, C.L., Marshall, A.G.: Predator Data Station: a fast data acquisition system for advanced FT-ICR MS experiments. Int. J. Mass Spectrom. **306**, 246–252 (2011)
33. Jiao, C.Q., Ranatunga, D.R.A., Vaughn, W.E., Freiser, B.S.: A pulsed-leak valve for use with ion trapping mass spectrometers. J. Am. Soc. Mass Spectrom. **7**, 118–122 (1996)
34. Jones, C.A., Dearden, D.V.: Linewidth pressure measurement: a new technique for high vacuum characterization. J. Am. Soc. Mass Spectrom. **26**, 323–329 (2015)
35. Mesleh, M., Hunter, J., Shvartsburg, A., Schatz, G., Jarrold, M.: Structural information from ion mobility measurements: effects of the long-range potential. J. Phys. Chem. **100**, 16082–16086 (1996)
36. Shvartsburg, A.A., Jarrold, M.F.: An exact hard-spheres scattering model for the mobilities of polyatomic ions. Chem. Phys. Lett. **261**, 86–91 (1996)
37. Shvartsburg, A.A., Hudgins, R.R., Dugourd, P., Jarrold, M.F.: Structural elucidation of fullerene dimers by high-resolution ion mobility measurements and trajectory calculation simulations. J. Phys. Chem. A **101**, 1684–1688 (1997)
38. Shvartsburg, A.A., Pederson, L.A., Hudgins, R.R., Schatz, G.C., Jarrold, M.F.: Structures of the clusters produced by laser desorption of fullerenes: [2 + 2] cycloadducts of preshrunk cages. J. Phys. Chem. A **102**, 7919–7923 (1998)
39. Shvartsburg, A.A., Mashkevich, S.V., Baker, E.S., Smith, R.D.: Optimization of algorithms for ion mobility calculations. J. Phys. Chem. A **111**, 2002–2010 (2007)
40. Alizadeh, N., Shahdousti, P., Nabavi, S., Tabrizchi, M.: Atmospheric pressure gas-phase ammonium/alkyl ammonium exchange studies of some crown ethers complexes using ion mobility spectrometry: a thermodynamic investigation and collision cross-section measurements. Int. J. Mass Spectrom. **308**, 18–25 (2011)
41. Davidson, K.L., Bush, M.F.: Effects of drift gas selection on the ambient-temperature, ion mobility mass spectrometry analysis of amino acids. Anal. Chem. **89**, 2017–2023 (2017)
42. Ridge, D.P., Beauchamp, J.L.: Interaction of ions with nonpolar neutrals – collision broadening of ion-cyclotron resonance lines of ions in hydrogen and methane. J. Chem. Phys. **64**, 2735–2746 (1976)
43. Lee, S., Wyttenbach, T., von Helden, G., Bowers, M.T.: Gas phase conformations of Li^+, Na^+, K^+, and Cs^+ complexed with 18-crown-6. J. Am. Chem. Soc. **117**, 10159–10160 (1995)
44. von Helden, G., Wyttenbach, T., Bowers, M.T.: Conformation of macromolecules in the gas phase: use of matrix-assisted laser desorption methods in ion chromatography. Science **267**, 1483–1485 (1995)
45. Creaser, C., Griffiths, J., Stockton, B.: Gas-phase ion mobility studies of amines and polyether/amine complexes using tandem quadrupole ion trap/ion mobility spectrometry. Eur. J. Mass Spectrom. **6**, 213–218 (2000)
46. Kralj, M., Tusek-Bozic, L., Frkanec, L.: Biomedical potentials of crown ethers: prospective antitumor agents. ChemMedChem **3**, 1478–1492 (2008)
47. Hilderbrand, A.E., Myung, S., Clemmer, D.E.: Exploring crown ethers as shift reagents for ion mobility spectrometry. Anal. Chem. **78**, 6792–6800 (2006)
48. Hariharan, C., Ingo Baumbach, J., Vautz, W.: Empirical prediction of reduced ion mobilities of secondary alcohols. Int. J. Ion Mobil. Spectrom. **12**, 59–63 (2009)
49. Hariharan, C.B., Baumbach, J.I., Vautz, W.: Linearized equations for the reduced ion mobilities of polar aliphatic organic compounds. Anal. Chem. **82**, 427–431 (2010)
50. Ahmed, A., Cho, Y.J., No, M., Koh, J., Tomczyk, N., Giles, K., Yoo, J.S., Kim, S.: Application of the Mason-Schamp equation and ion mobility mass spectrometry to identify structurally related compounds in crude oil. Anal. Chem. **83**, 77–83 (2011)
51. Dhungana, B., Becker, C., Chambliss, C.K.: The influence of terminal group and repeat unit structure on mass-mobility correlations observed for homologous series. Int. J. Ion Mobil. Spectrom. **19**, 57–64 (2016)
52. Newell, A.C., Baird, R.C.: Absolute determination of refractive indices of gases at 47.7 gigahertz. J. Appl. Phys. **36**, 3751–3759 (1965)
53. Hohm, U., Kerl, K.: Interferometric measurements of the dipole polarizability α of molecules between 300 K and 1100 K. I. Monochromatic measurements at $\Lambda = 632.99$ Nm for the noble-gases and H_2, N_2, O_2, and CH_4. Mol. Phys. **69**, 803–817 (1990)
54. Hohm, U., Kerl, K.: Interferometric measurements of the dipole polarizability A of molecules between 300 K and 1100 K. II. A new method for measuring the dispersion of the polarizability and its application to Ar, H_2, and O_2. Mol. Phys. **69**, 819–831 (1990)
55. Alvarez, S.: A cartography of the van der Waals territories. Dalton Trans. **42**, 8617–8636 (2013)
56. Phelps, A., Greene, C., Burke, J.: Collision cross-sections for argon atoms with argon atoms for energies from 0.01 eV to 10 keV. J. Phys. B-At. Mol. Opt. Phys. **33**, 2965–2981 (2000)
57. Haynes, W.M. (ed.): CRC handbook of chemistry and physics. CRC Press, Boca Raton (2016)
58. Kemper, P.R., Dupuis, N.F., Bowers, M.T.: A new, higher resolution, ion mobility mass spectrometer. Int. J. Mass Spectrom. **287**, 46–57 (2009)